Influence of the CO_2 Antisolvent Effect on Ultrasound-Induced Polymer Scission Kinetics

Martijn W. A. Kuijpers, Ramona M. H. Prickaerts, Maartje F. Kemmere,* and Jos T. F. Keurentjes

Process Development Group, Department of Chemical Engineering & Chemistry, Eindhoven University of Technology, P.O. Box 513, 5600 MB Eindhoven, The Netherlands

Received June 4, 2004; Revised Manuscript Received December 3, 2004

ABSTRACT: Ultrasound-induced polymer scission is a nonrandom process which alters the molecular weight distribution of polymers. However, transient cavitation, and consequently polymer scission, is not possible in concentrated polymer solutions due to the high liquid viscosity. The addition of an antisolvent can be used to circumvent this problem because the antisolvent decreases the gyration radius of polymer chains, which induces a reduction in liquid viscosity. To determine the influence of carbon dioxide (CO_2) as an antisolvent on the ultrasound-induced scission rate, ultrasonic scission experiments of poly(methyl methacrylate) have been performed in bulk methyl methacrylate (MMA) as well as in CO_2-expanded MMA. Modeling the experimental time-dependent molecular weight distributions (MWD) has revealed the scission kinetics at different polymer concentrations and CO_2 fractions. At low polymer concentrations, the scission rate is decreased upon an increased CO_2 content. This is a result of the higher vapor pressure of CO_2, which cushions the cavitation. However, at higher polymer concentrations, this effect is counteracted by the viscosity reduction induced by CO_2. As a consequence, the scission rate in CO_2-expanded MMA is higher as compared to bulk MMA for solutions with a high polymer concentration. The results show that ultrasound-induced scission in pressurized CO_2 can alter and control the MWD of polymers even in concentrated polymer solutions, whereas ultrasound-induced scission in bulk solutions is limited to relatively low polymer concentrations.

Introduction

The molecular weight distribution (MWD) is an important characteristic of polymers. In the polymer industry, a postprocessing step is often applied to alter the MWD, e.g., peroxide-induced degradation of polypropylene.[1] In this process, fracture of the polymer chains occurs at random sites. An alternative method is ultrasound-induced polymer scission, which involves a much better controlled, nonrandom process.[2] It can either be used as a postprocessing step or can be used during ultrasound-induced polymerizations.[3]

Ultrasound is known to enhance chemical reactions, as well as mass transfer, at ambient temperatures and pressures. Most of these effects are caused by transient cavitations, i.e., the collapse of microscopic bubbles in a liquid. The chemical effects of cavitation result from the extreme conditions in the bubble (5000 K and 200 bar)[4] and the high strain rates outside the bubble (10^7 s^{-1})[5] generated upon implosion. Polymer scission arises from the high strain rates near an imploding cavity. The chain is fractured approximately in the middle of the chain, until a limiting molecular weight (M_{lim}) is reached.[6] The M_{lim} is defined as the maximum chain length that does not break by ultrasound. A direct consequence of the nonrandom scission behavior is that no oligomers are formed by ultrasound-induced scission, in contrast to chemical degradation of polymers. Oligomers often have a negative influence on the polymer properties and are thus undesired in the final product. Additionally, an interesting application of ultrasound-induced polymer scission is the production of block copolymers, for which two different methods are possible. The first route involves the dissolution of a homopolymer in a different monomer.[7] Subsequently, ultrasonic scission of the polymer chains will generate the radicals that initiate the polymerization reaction with the monomer present. In the second method, two different homopolymers are dissolved in a nonreactive solvent.[8] Ultrasound generates polymeric radicals, which will terminate by cross combination. The advantage of this method is that block copolymers can be produced from homopolymers of which the polymer−monomer systems are immiscible. For the system considered in this study, poly(methyl methacrylate) (PMMA) radicals react with a radical scavenger. In experiments without radical scavenger present, PMMA radicals would terminate by disproportionation.

Typically, polymer scission experiments are performed in the corresponding monomer as the solvent. Several studies have considered the solvent quality during scission experiments,[9,10] for which an increased degradation rate and a decreased M_{lim} have been observed when better solvents are used. In the literature, these effects have been ascribed to the configuration of the polymer chain, which becomes more open in better solvents. Additionally, some correlation with the χ parameter has been observed.

The viscosity is an important factor during ultrasound-induced scission.[11] A high viscosity hinders both the growth of a cavity, as well as the collapse of a cavity, and consequently, the polymer scission rate is reduced. At increasing polymer concentration, the scission process is less effective and eventually stops, as a high viscosity hinders the bubble implosion. This is a drawback for the development of a scission process based on ultrasound, as concentrated polymer systems are favored in industry. The addition of an antisolvent for the polymer can counteract the increase in viscosity at

* Author to whom correspondence should be addressed. E-mail: M. F.Kemmere@TUE.nl.

10.1021/ma048895d CCC: $30.25
Published on Web 01/25/2005

higher polymer concentrations.[12] At relatively low antisolvent concentrations, the viscosity reduction is a result of the smaller gyration radius of the dissolved polymer molecules. It is still a one-phase system, due to which, the scission rate constant is expected to remain virtually unchanged. At higher CO_2 fractions, the polymer precipitates, and as a result, a second phase is formed. The precipitated polymer cannot be stretched by cavitation, and subsequently, it is no longer susceptible for ultrasound-induced scission. A constant scission rate is thus expected with increasing polymer concentration, as the liquid viscosity is unchanged by precipitation of the polymer.

High-pressure CO_2 is an interesting medium for ultrasound-induced polymer scission because it exhibits an antisolvent effect for most polymers, whereas most monomers have a high solubility in CO_2.[13] As a consequence, a CO_2-based process allows for relative easy separation of the polymer product from the reaction medium. Moreover, CO_2 is regarded as an environmentally friendly compound that is nontoxic, nonflammable, and naturally abundant.[14,15] However, up till now, ultrasound has rarely been studied at higher pressures because in most cases a high static pressure hampers the growth of cavities. Recently, we have shown that transient cavitation is possible in dense-phase fluids.[16] This provides a means for the development of scission processes based on ultrasound and high-pressure CO_2. These types of processes can contribute to a safer and cleaner way to produce polymers with the desired MWD. By adjusting the CO_2 fraction in the liquid, the amount of polymer that is dissolved can be controlled and, hence, the scission rate. Moreover, the CO_2 fraction influences the liquid viscosity and the vapor pressure, which determine the cavitation intensity.[2] Therefore, the cavitational collapse, and consequently, the fracture rate and the M_{lim} are dependent on the amount of CO_2 in the liquid.

In this work, the influence of the CO_2 antisolvent effect on the ultrasound-induced polymer scission has been studied. Scission experiments have been performed at different CO_2 fractions and polymer concentrations. With the development of the experimental MWDs, as well as a general scission model based on population balances, the influence of CO_2 and the polymer concentration on the scission kinetics have been determined.

Ultrasound-Induced Scission. The breakage of polymer molecules due to ultrasound is a direct result of transient cavitation because no polymer fracture occurs when cavitation is suppressed.[17] Upon bubble collapse, the entire molecule moves along with the fluid. Due to the velocity profile near the cavities, friction between the polymer chain and the liquid occurs (Figure 1). This friction can result in stretching of the polymer coil and subsequent fracture of the chain. As described in a previous paper, the breaking of the polymer chain appears to be the rate-limiting step, not the stretching of the chain.[18] Since the drag force accumulates in the middle of the chain, scission primarily occurs at the center because the chance to break is the largest in the middle of the polymer chain. Of course, multiple breakage can occur during one scission experiment. However, it is not possible to remove a small fragment from a long polymer chain by ultrasound-induced scission because the forces acting on that bond are too small. The chain is fractured if the accumulated drag force in a chain fragment is higher than the bond strength. This force

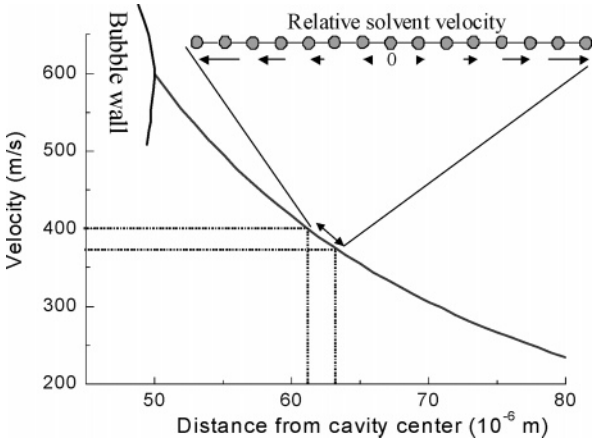

Figure 1. Schematic representation of the velocity profile near an imploding bubble and the resulting relative liquid velocity near a stretched polymer chain.

(eq 1) is dependent on the size of the monomer molecules (a and b represent the radius and the length of a monomeric unit in a polymer chain,[18] respectively), the shielding factor (S), the solvent viscosity (η), the number of monomer units (n), and the strain rate ($d\epsilon/dt$).[19] The strain rate can be calculated from the distance of the polymer chain from the center of the cavity (r), the bubble wall velocity (dR/dt), and the radius of the bubble (R) (eq 2).[20]

$$F_c = \frac{6\pi}{8}\eta a b S \frac{d\epsilon}{dt} n^2 \tag{1}$$

$$\frac{d\epsilon}{dt} = -2\frac{R^2 \frac{dR}{dt}}{r^3} \tag{2}$$

The two most important quantities describing an ultrasound-induced scission reaction are the M_{lim} and the scission rate. The first is determined by the maximum strain rate in the liquid, which is obtained at the cavity interface at the moment of implosion. From the cavitation bubble interface toward the bulk liquid, the strain rate decreases rapidly. Polymer chains with a molecular weight slightly higher than M_{lim} can only break in the vicinity of the bubble interface, whereas higher-molecular-weight polymers can also break further away from the cavitation bubble. The scission rate is thus proportional to the volume around the cavity in which a polymer chain can stretch and break. Since the strain rate and the length of the polymer chain determine this volume, relatively low-molecular-weight polymers have a small volume in which they can break and, hence, have a low scission rate. The scission volume increases for polymer chains with a higher molecular weight and for faster imploding bubbles. The kinetics of ultrasonic scission can thus be directly ascribed to the implosion velocity of the cavitation bubbles and the length of the polymer that is fractured. The implosion velocity is dependent on the liquid properties, the content of the bubble, the acoustic pressure, and the static pressure, respectively.[21] Therefore, it is important to know the phase composition, density, and viscosity of the liquid.

Assuming first-order scission kinetics, the scission rate can be determined as a function of molecular weight

and liquid properties. The kinetic scheme of scission by ultrasound reads as follows[22]

$$\text{Scission:} \quad P_n \xrightarrow{k_d(n,m)} P_m^{\bullet} + P_{n-m}^{\bullet}$$

Termination by

$$\text{recombination:} \quad P_m^{\bullet} + P_{n-m}^{\bullet} \xrightarrow{k_{tc}} P_n$$

Termination by

$$\text{disproportionation:} \quad P_m^{\bullet} + P_{n-m}^{\bullet} \xrightarrow{k_{td}} P_m + P_{n-m}$$

If a radical scavenger is present, the termination reaction occurs instantaneously only between a macroradical fragment and a scavenger molecule. Thus, the scheme reduces to

$$P_n \xrightarrow{k_d(n,m)} P_m + P_{n-m}$$

where $k_d(n,m)$ is an effective scission rate constant. The scission rate constant k_d is chosen as a function of the original chain length, n, and fragment length, m, to allow for the nonrandom character of the scission process. According to the overall scission reaction, the population balance then becomes

$$\frac{dP_n}{dt} = \sum_{m=n+1}^{\infty} k_d(n,m)P_m - P_n \sum_{m=1}^{n} k_d(n,m) \qquad (3)$$

This balance equation is solved with the Galerkin finite element (FEM) package PREDICI.[23] By manipulating the shape of $k_d(n,m)$, which is anticipated to be Gaussian with a width (σ), it is possible to obtain a best fit between the MWD predicted by eq 4 and the measured MWD. The overall dissociation constant k_d consists of a Gaussian distribution function and a molecular-weight-dependent scission function (k_{MW}):[18]

$$k_d(n,m) = \frac{k_{MW}(n)}{\sqrt{2\pi}\sigma(n)} e^{\left(-\frac{1}{2\sigma(n)^2}\left(m-\frac{n}{2}\right)^2\right)} \qquad (4)$$

As the force in the middle of the chain has a squared dependence in the number of monomeric units (eq 1), an almost quadratic function is used to describe the dissociation rate as a function of the molecular weight (eq 5). This equation is only valid for polymer chains with a molecular weight higher or equal to M_{lim}. When the dissociation constant k_{MW} is zero, the corresponding M_{lim} at these conditions is obtained. This molecular weight is determined by the constants A and B. The scission rate is defined by all three constants in eq 5:[18]

$$k_{MW}(n) = A + Bn^{2e^{-n/C}} \qquad (5)$$

Experimental Section

Materials. The polymer solutions used for the scission experiments with ultrasound consisted of MMA (Merck), CO_2 (grade 5.0, Hoekloos), and PMMA (self-made, M_w and polydispersity 2.4×10^6 g/mol and 2.4, respectively). The MMA was distilled under vacuum to remove the hydroquinone inhibitor before use. To ensure that no reaction or recombination of polymer radicals could occur during the scission experiments, a radical scavenger (1,1-diphenyl-2-picrylhydrazyl, Aldrich) was added to the solution.

The composition of the liquid was calculated with the Lee–Kessler–Plöcker (LKP) equation of state (Table 1).[24] In previous papers,[25,26] it was shown that the LKP-eos is the most suitable equation of state to describe CO_2-monomer systems. The LKP model uses pure component parameters, such as the critical temperature, the critical pressure, and the acentric factor (ω), and one binary interaction parameter. The interaction parameter for the MMA/CO_2 system appears to be 1.08 at 20 °C.[27] The influence of the polymer on the CO_2 fraction (X_{CO_2}) in the liquid at a certain pressure was assumed to be negligible. The density of the liquid was approximately 0.945 kg/L at 20 °C.[24]

Table 1. Experimental Conditions for the Ultrasound-Induced Scission Experiments[a]

T (°C)	P (bar abs)	X_{CO_2}	I_{US} (W/cm^2)
20	1.0	0.02	31
20	4.0	0.08	59
20	7.0	0.14	70

[a] The CO_2 fraction (X_{CO_2}) of the liquid was calculated with the Lee–Kessler–Plöcker equation of state.

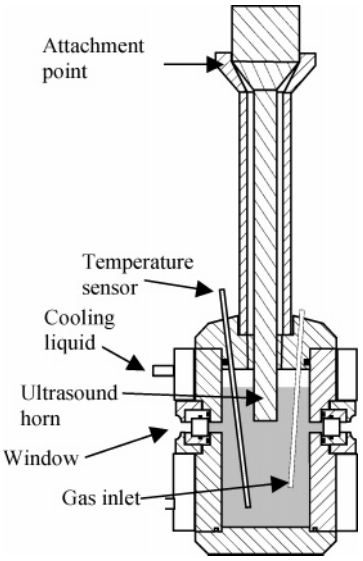

Figure 2. High-pressure ultrasound reactor for scission reactions.

Scission Experiments. Ultrasound-induced scission was studied in a thermostated 175 mL high-pressure vessel at 20 °C (Figure 2). Sonification of the solution was performed using 20 kHz ultrasound, which was produced by a Sonics and Materials VC-750 generator. A 1/2-in. full-wave titanium probe was applied to couple the piezoelectric transducer to the liquid. To allow for an accurate comparison, the total configuration and the ultrasound amplitude (75 μm) were kept constant during all the experiments.

The experimental procedure of the ultrasound-induced scission experiments was as follows. The reactor was filled with 150 mL of bulk MMA or CO_2-expanded MMA, in which a known amount of PMMA was dissolved. To ensure the presence of nuclei for cavitation bubbles, CO_2 was bubbled through a 3-mm tube into the reaction mixture with a flow rate of 2.0 mL/s during the experiments. This bubbling did not strip the MMA from the liquid phase because a condenser was placed on top of the reactor. As a result of the high solubility of CO_2 in MMA, bubbling CO_2 through bulk MMA at atmospheric conditions already resulted in a CO_2 fraction of 0.02 (Table 1). In the CO_2-expanded MMA systems, a two-phase system was applied. The CO_2 gas phase was in equilibrium with the liquid CO_2/MMA phase. By adjusting the CO_2 pressure, the fraction of CO_2 could be controlled.

Analysis. During the scission reaction, samples were taken and analyzed by gel permeation chromatography (GPC), which was calibrated against polystyrene standards. The MWDs of the PMMA samples were calculated with Mark–Houwink parameters ($a = 0.719$ and $K = 9.44 \times 10^{-5}$ m^3).[28] The modeling procedure for the MWDs was as follows: the

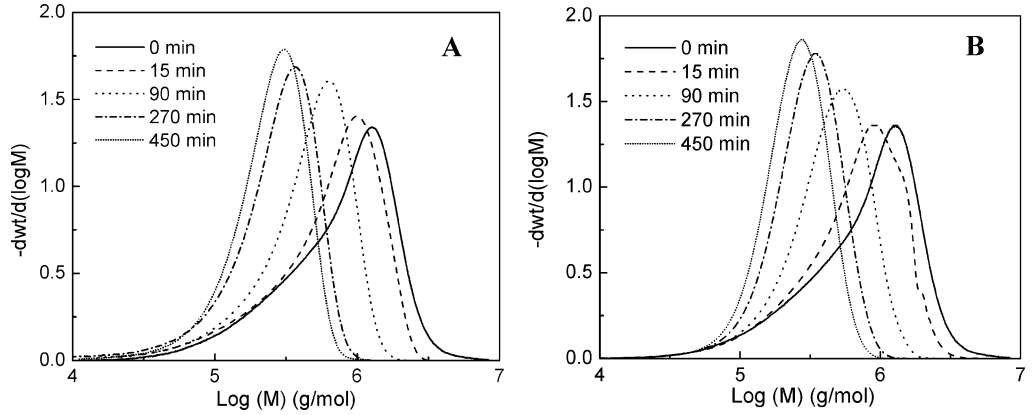

Figure 3. Experimental (A) and simulated (B) molecular weight distributions of an ultrasound-induced scission reaction of 4 wt% PMMA in bulk MMA ($X_{CO_2} = 0.02$).

Table 2. Experimental and Modeling Results of Ultrasound-Induced Scission in Bulk MMA (X_{CO_2}= 0.02) at Different Polymer Concentrations

wt% PMMA	X_{CO_2}	$M_{lim,experiment}$ (10^5 g/mol)	$M_{lim,model}$ (10^5 g/mol)	A (10^{-5} 1/s)	B (10^{-11} 1/s)	C (10^6)	$2e^{-n/C}$ at 10^6 g/mol
0.1	0.02	1.0	0.9	-2 ± 1	$2.4 + 0.1$	$0.2 + 0.1$	1.9
2.0	0.02	1.9	0.9	$-0.1 + 0.1$	$0.13 + 0.01$	5 ± 1	2
4.0	0.02	1.9	1.0	$-0.1 + 0.1$	$0.10 + 0.01$	5 ± 1	2

experimentally obtained MWDs were fitted using PREDICI. The applied model in this fitting procedure is described in detail in a previous paper.[18] In this way, the molecular-weight-dependent scission rate constants ($k_d(n,m)$) could be determined on the basis of the constants A, B, and C (see eq 5). Subsequently, the M_{lim} was calculated and compared with the experimentally observed M_{lim}.

The ultrasound intensities were determined at an amplitude of 75 μm for the different conditions by calorimetry and are given in Table 1. These values give an indication of the ultrasound power transferred to the liquid in the high-pressure reactor. The heat flow (Q) that was generated by ultrasound in the calorimeter was calculated on the basis of the surface area of the reactor wall (A_r), the overall heat transfer coefficient (U), and the difference between jacket (T_j) and reactor temperature (T_r).[27] Subsequently, the ultrasound intensity (I_{US}), was calculated by dividing the heat flow by the surface area of the ultrasound horn (A_{US}) according to eq 6.[30]

$$I_{US} = \frac{Q}{A_{US}} = \frac{UA_r(T_r - T_j)}{A_{US}} \tag{6}$$

Results and Discussion

In this study, the effect of the CO_2 fraction and the polymer concentration on the scission kinetics has been determined by comparing experimentally obtained MWDs with fitted MWDs using PREDICI. First, the ultrasound-induced polymer scission simulations will be discussed briefly. Next, the influence of the liquid viscosity on the scission kinetics has been determined in bulk MMA. To quantify the influence of CO_2 on the implosion velocity independently from the CO_2 antisolvent effect, first, the influence of the CO_2 fraction on the fracture rate has been measured at low polymer concentrations. Subsequently, the antisolvent effect of CO_2 on the scission kinetics has also been studied for more concentrated polymer solutions. Finally, the application of CO_2 to control the molecular weight during ultrasound-induced scission is discussed.

Simulations of Ultrasound-Induced Polymer Scission. Figure 3A shows the development of the MWD for a scission experiment in bulk with 4 wt% PMMA. A decrease in polydispersity and molecular weight is obtained by irradiation of the solution with ultrasound. The modeled MWDs for this scission reaction are shown in Figure 3B. In a previous study, where monodisperse polymer samples have been used in bulk MMA, the width of the sigmoidal distribution function (eq 4) has been determined, which appears to be $\sigma(n) = 0.13n$.[18]

In general, the model describes the scission reaction well, as only minor differences between the experimental and the model results can be observed. The calculated MWD for $t = 15$ min shows a shoulder at the high-molecular-weight side. This is caused by the grid division in PREDICI because the calculation steps increase at higher molecular weight. Table 2 presents the limiting molecular weight and the constants and the exponent for the scission rate constant $k_{MW}(n)$ as given in eq 5.

Influence of Viscosity on Transient Cavitation. The liquid viscosity has a major influence on the implosion velocity and, consequently, on the scission rate and M_{lim}. The experimentally observed development of M_w at different polymer concentrations in bulk MMA is plotted in Figure 4A. In contrast to the solutions with 2.0 and 4.0 wt%, the low polymer concentration of 0.1 wt% is below entanglement and the coils of the polymer chains do not touch each other. Figure 4B shows the scission constants (k_d), determined by the simulations as a function of molecular weight at different polymer concentrations in bulk MMA. It should be noted that, with decreasing molecular weights, the reaction time increases. A much lower scission rate constant is observed at higher polymer concentrations, which is a result of the higher viscosity. This decrease is the most distinct between polymer concentrations of 0.1 and 2 wt%, whereas the difference between 2 and 4 wt% dissolved polymer is small. Limiting molecular weights of 1.0×10^5, 1.9×10^5, and 1.9×10^5 g/mol are obtained for scission in bulk MMA for PMMA at concentrations of 0.1, 2, and 4 wt%, respectively (Table 2).

With respect to simulations using PREDICI, Table 2 shows that the calculated M_{lim} value at low polymer

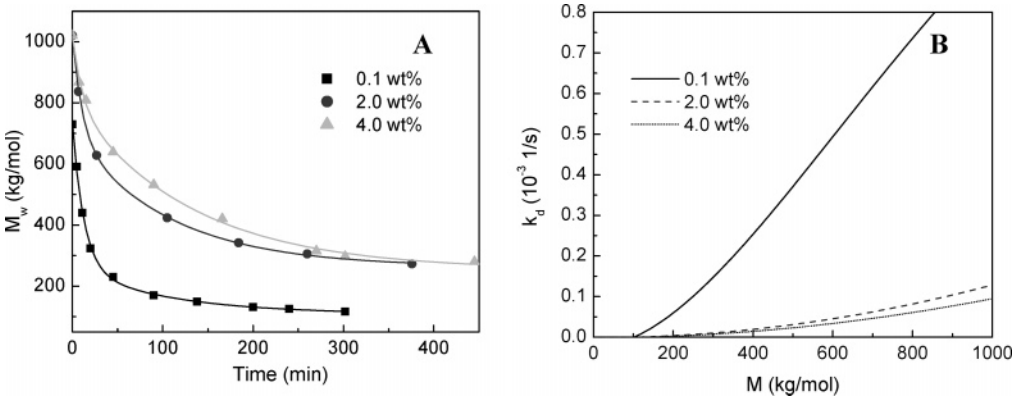

Figure 4. Experimentally observed development of the weight average molecular weight (A) and calculated scission rate constants (B) for ultrasound-induced scission at different PMMA concentrations in bulk MMA ($X_{CO_2} = 0.02$).

concentration is in good agreement with the experiment because the viscosity and, consequently, the cavitation intensity do not change during the experiment. Due to these constant experimental conditions, the scission model accurately predicts M_{lim} at low polymer concentrations. In contrast, at high polymer concentrations, the calculated M_{lim} values deviate from the experimentally obtained M_{lim}, approximately by a factor of 2. This is caused by the constant cavitation intensity in time used in the PREDICI model. This would imply that the viscosity of the solution remains constant during sonification. Experimentally, however, the viscosity changes significantly during the scission experiments of the more concentrated polymer solutions, as a result of which, the largest deviation in predicted M_{lim} is observed at the 2 and 4 wt% polymer solutions. In contrast to M_{lim}, the scission model accurately predicts the initial scission rate constants at higher polymer concentrations.

In Table 2, the molecular-weight-dependent scission constants at different polymer concentrations are given. The exponent ($2e^{-n/C}$) given in Table 2 describes the dependence of the scission rate on the chain length (eq 5). The scission rate is expected to be a quadratic function of the length of the chain (eq 1). Although this is correct for low-molecular-weight polymers, from the simulations with 0.1 wt% polymer, it is concluded that for higher-molecular-weight polymers (10^6 g/mol), the scission rate depends on the chain length to the power 1.9 (Table 2). This difference is significant, as described previously.[18] We assume that this deviance is probably a consequence of overlapping velocity profiles from neighboring cavitation bubbles (Figure 5). As a result, the volume in which a polymer with a certain molecular weight can break is reduced. The scission rate of a polymer chain is proportional to this volume, as mentioned in the theoretical section. In general, high-molecular-weight polymers can fracture further away from the bubble interface, and therefore, their scission rate will be more susceptible to this volume decrease. Consequently, the deviation from the theory (a quadratic function) is more distinct at higher molecular weights. Additionally, at higher cavitation intensities (lower viscosities), the radial velocity profile extends further in the liquid, which will cause more overlap with neighboring bubbles and, thus, a larger decrease in effective volume. As a result, a less-than-quadratic function is obtained at lower polymer concentrations.

Influence of CO_2 Fraction on Transient Cavitation. The influence of the CO_2 fraction on the implosion velocity has been measured independently from the antisolvent effect by performing the experiments at low polymer concentrations (Table 3). At low polymer concentrations, the influence of the CO_2 fraction on the viscosity can be neglected because the polymer chains are not entangled. Figure 6A shows the development of M_w in time for scission experiments with a low polymer concentration at different CO_2 fractions. With an increasing CO_2 fraction, the scission rate decreases (slope of Figure 6A) and the M_{lim} increases. The change in scission kinetics is a result of the lower strain rate produced upon collapse at higher CO_2 fractions. This is not an antisolvent effect because the CO_2 fraction has almost no influence on the viscosity in a 0.1 wt% polymer solution. However, the lower scission rate and higher M_{lim} at higher CO_2 pressures is a result of the higher vapor pressure in the cavitation bubble, which reduces the implosion velocity (cushioning effect) and, consequently, reduces the drag force acting on the polymer chain, see eq 1.

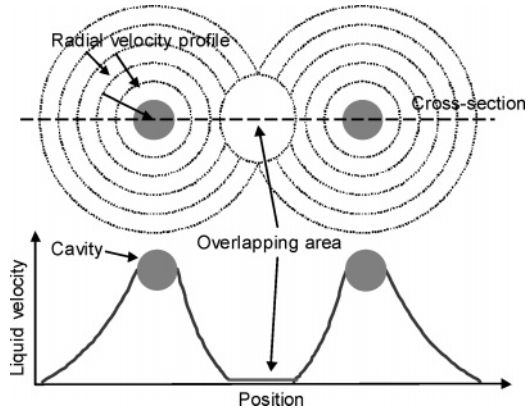

Figure 5. Schematic representation of overlapping velocity profiles around two imploding cavitation bubbles and the resulting radial velocity.

Figure 6B presents the overall scission constants at different CO_2 fractions as a function of the molecular weight. From the simulations, it is concluded that for higher-molecular-weight polymers (10^6 g/mol) the scission rate depends on the chain length to the power 1.9, 1.93, and 2 at 1, 4, and 7 bar, respectively (Table 3). This deviance from the theory is probably a consequence of overlapping velocity profiles from neighboring cavitation bubbles (Figure 5), as mentioned in the previous section. The larger deviation at lower pressures is caused by the higher implosion velocities. At lower CO_2 fractions, the radial velocity profile extends further in the liquid, which will cause more overlap with neigh-

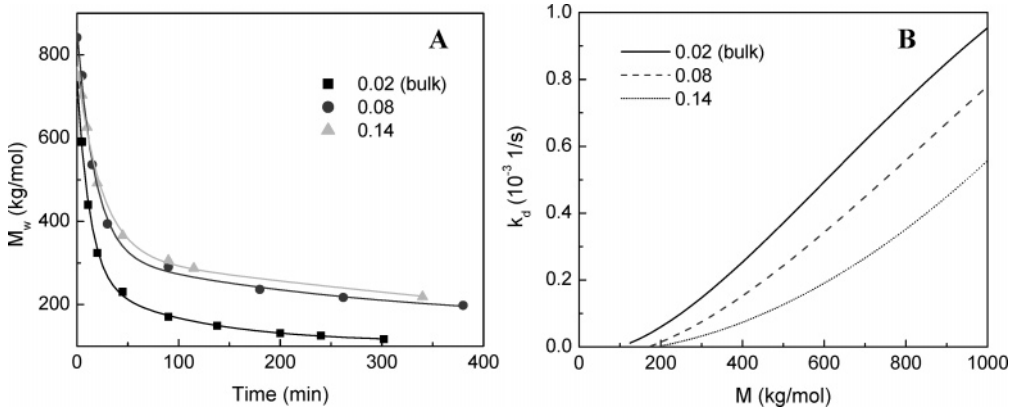

Figure 6. Experimentally observed development of the weight average molecular weight (A) and calculated scission rate constants (B) for ultrasound-induced scission at 0.1 wt% polymer and CO_2 fractions of 0.02, 0.08, and 0.14.

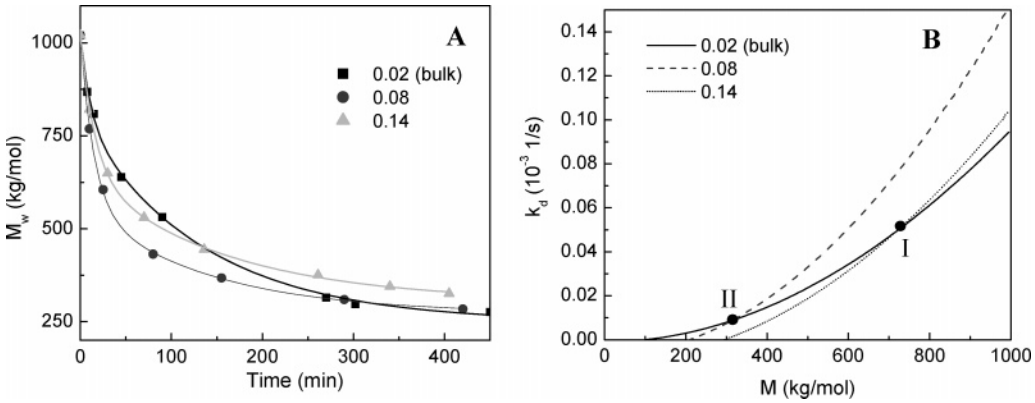

Figure 7. Experimentally observed development of the weight average molecular weight (A) and calculated scission rate constants (B) for ultrasound-induced scission at 4.0 wt% polymer and CO_2 fractions of 0.02, 0.08, and 0.14.

Table 3. Experimental and Modeling Results of Ultrasound-Induced Scission at Different CO_2 Fractions and 0.1 wt% Polymer

wt% PMMA	X_{CO_2}	$M_{lim,experiment}$ (10^5 g/mol)	$M_{lim,model}$ (10^5 g/mol)	A (10^{-5} 1/s)	B (10^{-11} 1/s)	C (10^6)	$2e^{-n/C}$ at 10^6g/mol
0.1	0.02	1.0	0.9	-2 ± 1	$2.4 + 0.1$	$0.2 + 0.1$	1.9
0.1	0.08	1.6	1.6	-4 ± 1	$1.5 + 0.1$	$0.3 + 0.1$	1.93
0.1	0.14	1.8	1.8	-2 ± 1	$0.60 + 0.01$	5 ± 1	2

Table 4. Experimental and Modeling Results of Ultrasound-Induced Scission at Different CO_2 Fractions and 4.0 wt% Polymer

wt% PMMA	X_{CO_2}	$M_{lim,experiment}$ (10^5 g/mol)	$M_{lim,model}$ (10^5 g/mol)	A (10^{-5} 1/s)	B (10^{-11} 1/s)	C (10^6)	$2e^{-n/C}$ at 10^6 g/mol
4.0	0.02	1.9	1.0	$-0.1 + 0.1$	$0.10 + 0.01$	5 ± 1	2
4.0	0.08	2.6	2.1	$-0.7 + 0.1$	$0.16 + 0.01$	∞	2
4.0	0.14	3.0	2.9	-1 ± 1	$0.12 + 0.01$	∞	2

boring bubbles and, thus, results in a larger decrease in effective volume.

Influence of the Antisolvent Effect on the Scission Kinetics. Carbon dioxide reduces the viscosity of concentrated polymer solutions due to the antisolvent effect,[13] which induces a smaller gyration radius of the polymer or even polymer precipitation at higher CO_2 fractions. As a result, the scission rate constant is expected to remain virtually constant at higher polymer concentrations, whereas in bulk, the scission rate constant strongly decreases. Figure 7A shows the development of M_w in time for scission experiments for a 4 wt% polymer solution at several CO_2 fractions (Table 4). All the reaction mixtures are one-phase systems, as no precipitated polymer was observed in a high-pressure view-cell at these conditions. Figure 7B shows the scission rate constants for different CO_2 fractions, as obtained from the model. It can be seen that the scission rate constant is initially (the right-hand side of point I and the right-hand side of point II) higher for the CO_2-expanded liquids, in contrast to the bulk experiment (Figure 7B vs 6B). The negative influence of the CO_2 fraction on the implosion velocity at low polymer concentrations is thus counteracted at higher polymer concentrations by the CO_2 antisolvent effect. As no precipitated polymer is observed, the higher scission rate is a consequence of the smaller gyration radius of the polymer chain, which results in a lower liquid viscosity. At the left-hand side of point I in Figure 7B, the scission rate in bulk is faster than the scission rate in CO_2-expanded MMA at 7 bar ($X_{CO_2} = 0.14$). The difference with the right-hand side is caused by the larger viscosity decrease during the scission experiment in bulk MMA, which results in a larger increase in the

implosion velocity of the cavitation bubbles. This higher implosion velocity also results in a lower M_{lim} for the scission experiment in bulk MMA as compared to scission in CO_2-expanded MMA. The intersection point between CO_2-expanded MMA at 4 bar ($X_{CO_2} = 0.08$) and bulk MMA (Figure 7B, II) occurs at a lower molecular weight because at 4 bar less CO_2 is dissolved in MMA, as compared to 7 bar. Therefore, the cushioning effect will be less pronounced at 4 bar CO_2.

As discussed in the previous sections, the CO_2 antisolvent effect and CO_2 cushioning effect have an opposite influence on the scission rate. Additionally, when substantial amounts of polymer are precipitated, it is possible that the breakage of polymer chains in solution is limited by the dissolution rate of the polymer from the precipitated phase. These effects may cause an optimum in scission rate at increasing static pressure.

Control of Molecular Weight by Ultrasound-Induced Polymer Scission. In general, ultrasound can be applied as a clean alternative method to control polymer properties by tuning the polydispersity and MWD because polymer scission occurs in situ without the addition of peroxides.[1] Especially for polymers where the high-molecular-weight part of the distribution has a disadvantageous effect on the product properties, ultrasound has significant application potential. The possibility to perform these reactions at higher polymer concentration by the addition of an antisolvent makes the ultrasound technique more feasible for industry. In another study,[31] a preliminary process design is presented for the production of 10 kg/h pure PMMA in CO_2-expanded MMA including polymer scission. This process appears to be especially interesting for the production of specialty products for biomedical purposes.

Moreover, by combining ultrasound with CO_2, the scission rate and M_{lim} can independently be altered. In comparison with bulk experiments, scission in CO_2-expanded liquids results in a lower viscosity and, consequently, a higher scission rate, as well as a lower M_{lim} in concentrated polymer solutions. Above a given CO_2 fraction, the polymer starts precipitating, resulting in a constant scission rate. The CO_2 fraction influences the amount of polymer that is dissolved, the M_{lim}, and the scission rate. Additionally, an increase in the ultrasound intensity will result in a lower M_{lim} and a higher scission rate, whereas the sonication area only influences the scission rate. In summary, the ultrasound intensity, the sonication area, and the CO_2 fraction can thus independently influence the limiting molecular weight and the scission rate. Therefore, ultrasound-induced polymer scission in CO_2-expanded liquids allows for an accurate control of the scission kinetics and, hence, the polymer properties.

Conclusions

In this work, the influence of the CO_2 antisolvent effect on the viscosity and the resulting reaction kinetics of ultrasound-induced polymer modification have been studied. For this purpose, ultrasound-induced polymer scission experiments have been performed in CO_2-expanded MMA, as well as in bulk MMA, at different PMMA concentrations. Modeling the development of the experimental MWDs in PREDICI has revealed the scission kinetics at different polymer and CO_2 concentrations. At low polymer concentrations, the scission rate decreases at higher CO_2 pressures due to the negative influence of CO_2 on the cavitation velocity. However, at higher polymer concentrations, this effect is counteracted by the viscosity reduction induced by the antisolvent effect of CO_2, which results in faster scission in CO_2-expanded MMA, as compared to bulk MMA. When CO_2 acts as an antisolvent, it is possible to alter the MWD of polymers by ultrasound in concentrated polymer solutions.

Acknowledgment. The authors thank the technical staff of the Department of Chemical Engineering and Chemistry, especially Chris Luyk, for the development and the construction of the high-pressure ultrasound vessel. The authors would also like to thank Wieb Kingma of the Polymer Chemistry Group for measuring the molecular weight distributions.

References and Notes

(1) Machado, A. V.; Covas, J. A.; Van Duin, M. *J. Appl. Pol. Sci.* **2001**, *81*, 58.
(2) Kuijpers, M. W. A.; Kemmere, M. F.; Keurentjes, J. T. F. Ultrasound-induced radical polymerization. In *Encyclopedia of Polymer Science and Technology*; John Wiley and Sons: New York, 2004.
(3) Price, G. J. *Ultrason. Sonochem.* **1996**, *3*, S229.
(4) Didenko, Y. T.; Mcnamara, W. B., III; Suslick, K. S. *Polymer* **1997**, *38*, 3783.
(5) Pestman, J. M.; Engberts, J. B. F. N.; De Jong, F. *Recl. Trav. Chim. Pays-Bas* **1994**, *113*, 533.
(6) Fujiwara, H.; Tanaka, J.; Horiuchi, A. *Polym. Bull.* **1996**, *36*, 723.
(7) Fujiwara, H. *Polym. Bull.* **2001**, *47*, 247.
(8) Madras, G.; Karmore, V. *Polymer Int.* **2001**, *50*, 683.
(9) Madras G.; Chattopadhyay, S. *Polym. Degrad. Stab*. **2001**, *71*, 273.
(10) Price, G. J.; West, P. J.; Smith, P. F. *Ultrason. Sonochem.* **1994**, *1*, S51.
(11) Kemmere, M. F.; Kuijpers, M. W. A.; Jacobs, L. J. M.; Keurentjes, J. T. F. *Macromol. Symp.* **2004**, *206*, 321.
(12) Shaffer, K. A.; DeSimone, J. M. *Trends Polym. Sci.* **1995**, *3*, 146.
(13) Jessop, P. G.; Leitner, W. *Chemical Synthesis using Supercritical Fluids*; Wiley-VCH: Weinheim, 1999.
(14) Abraham, M. A.; Moens, L. *Clean Solvents, Alternative Media for Chemical Reactions and Processing*; ACS Symposium Series 819; American Chemicl Society: Washington, DC, 2002.
(15) Kuijpers, M. W. A.; Van Eck, D.; Kemmere, M. F.; Keurentjes, J. T. F. *Science* **2002**, *298*, 1969.
(16) Mason, T. J.; Lorimer, J. P. *Applied Sonochemistry*; Wiley-VCH: Weinheim, 2002.
(17) Kuijpers, M. W. A.; Iedema, P. D.; Kemmere, M. F.; Keurentjes, J. T. F. *Polymer* **2004**, *45*, 6461.
(18) Odell, J. A.; Keller, A. *J. Pol. Sci. B* **1986**, *24*, 1889.
(19) Agarwal, U. S. *e-Polym.* **2002**, *14*, 1.
(20) Leighton, T. J. *The Acoustic Bubble*; Academic Press: London, 1994.
(21) Casale, A.; Porter, R. S. *Polymer Stress Reactions*; Academic Press: New York, 1978.
(22) Wulkow, M. *Macromol. Theory Simul.* **1996**, *5*, 393.
(23) Plöcker, U.; Knapp, H.; Prausnitz, J. *Ind. Eng. Chem. Process Des. Dev.* **1978**, *17*, 324.
(24) De Vries, T. J.; Kemmere, M. F.; Keurentjes, J. T. F. *Macromolecules* **2004**, *37*, 4241.
(25) Kemmere, M. F.; De Vries, T. J.; Keurentjes, J. T. F. In *Supercritical carbon dioxide in polymer reaction engineering*; Wiley-VCH: Weinheim, 2005.
(26) Kuijpers, M. W. A.; Jacobs, L. J. M.; Kemmere, M. F.; Keurentjes, J. T. F. *AIChE J*., in press.
(27) Xue, L.; Agarwal, U. S.; Lemstra, P. J. *Macromolecules* **2002**, *35*, 8650.
(28) Kuijpers, M. W. A.; Kemmere, M. F.; Keurentjes, J. T. F. *Ultrasonics* **2002**, *40*, 675.
(29) Hoffmann, U.; Horst, C.; Wietelmann, U.; Bandelin, S.; Jung, R. Sonochemistry. In *Ullmann's Encyclopedia of Industrial Chemistry*; Wiley-VCH: Weinheim, 2003.
(30) Kemmere, M. F.; Kuijpers, M. W. A.; Prickaerts, R. M. H.; Keurentjes, J. T. F. *Macromol. Mater. Eng.*, in press.

MA048895D